AIP | Journal of Applied Physics

Charge transport in amorphous low bandgap conjugated polymer/fullerene films

Jung Yong Kim, Hyunduck Cho, Seunguk Noh, Yoonkyoo Lee, Young Min Nam et al.

Citation: J. Appl. Phys. **111**, 043710 (2012); doi: 10.1063/1.3686633
View online: http://dx.doi.org/10.1063/1.3686633
View Table of Contents: http://jap.aip.org/resource/1/JAPIAU/v111/i4
Published by the American Institute of Physics.

Charge transport in amorphous low bandgap conjugated polymer/fullerene films

Jung Yong Kim,[1,a)] Hyunduck Cho,[2] Seunguk Noh,[2] Yoonkyoo Lee,[1] Young Min Nam,[1] Changhee Lee,[2,b)] and Won Ho Jo[1,c)]
[1]*Department of Materials Science and Engineering, Seoul National University, 599 Gwanak-ro, Gwanak-gu, Seoul, 151-742, South Korea*
[2]*School of Electrical Engineering and Computer Science, Inter-university Semiconductor Research Center, Seoul National University, 599 Gwanak-ro, Gwanak-gu, Seoul, 151-742, South Korea*

(Received 25 August 2011; accepted 16 January 2012; published online 23 February 2012)

The structural and charge transport properties of a low bandgap copolymer poly(3-hexylthiophene -*alt*-6,7-dimethyl-4,9-bis-(4-hexylthien-2yl)-[1,2,5]thiadiazolo[3,4-g]quinoxaline) (P(3HT-MeTDQ)) and its blend with [6,6]-phenyl-C_{61}-butyric acid methyl ester (PCBM) are investigated. Thermal analysis, X-ray scattering diffraction (XRD), atomic force microscopy and transmission electron microscopy (TEM) of P(3HT-MeTDQ) reveal that the polymer is amorphous in solid state. As the hole mobility of P(3HT-MeTDQ) was measured by the time-of-flight photoconductivity method, the mobility was 3.35×10^{-4} $cm^2/V\,s$, which is very comparable to that of semicrystalline poly(3-hexyl thiophene). When the mobility of amorphous P(3HT-MeTDQ) was analyzed according to the Gaussian disorder model, the polymer has the energetic and positional disorders with the values of $\sigma = 62$ meV and $\Sigma = 1.7$, respectively, indicating that the polymer has a relatively narrow Gaussian distribution of transport states. Interestingly, when P(3HT-MeTDQ) is blended with PCBM, the amorphous P(3HT-MeTDQ) becomes partially ordered, as evidenced by observation of two discernible XRD peaks at $2\theta = 5°$ ($d = 17.7$ Å) and 25.5° ($d = 3.5$ Å) corresponding to the interchain distance and π-stacking distance, respectively. The bicontinuous network morphology was identified at the blend with 60 wt. % PCBM by TEM, at which the charge carrier transport changes from hole-only to ambipolar. © *2012 American Institute of Physics*. [doi:10.1063/1.3686633]

I. INTRODUCTION

Blending a low bandgap conjugated polymer with a soluble fullerene is now a key strategy for enhancing the power conversion efficiency (PCE) of bulk-heterojunction organic photovoltaics (OPVs).[1–6] Recently, the National Renewable Energy Laboratory has certified the PCE of as high as 6.77% for a polymer/fullerene solar cell, in which the donor polymer is a poly(benzodithiophene-*alt*-thienothiophene) derivative with a bandgap of 1.77 eV and the lowest unoccupied molecular orbital (LUMO) = −3.45 eV.[5] Theoretically the design rule for achieving PCE of 10% has proposed that the ideal donor material must have a bandgap < 1.74 eV and $-4.0 \leq$ LUMO < −3.92 eV.[7] This calculation was based on the reports that the electron acceptor [6,6]-phenyl-C_{61}-butyric acid methyl ester (PCBM) has the LUMO of −4.3 eV and the donor/acceptor (D/A) LUMO offset should be at least larger than 0.3 eV.[7,8] Thus, the simple comparison of the best reported cell performance (PCE = 7.73%)[5] with the proposed design rule shows us that there is still room for improving toward a target of 10% efficiency.

For achieving better than the above-mentioned efficiency goal, we should not only develop new semiconducting polymers, but also understand the fundamental mechanism of the charge transport in conjugated polymer/fullerene blends and their devices.[4,6,9–13] The limiting factors governing the quantum efficiency of an OPV device are short-circuit current, open-circuit voltage, and fill-factor. These values are dependent strongly on photophysical properties of specific D/A material and its blending morphology.[14–16] However, phase behavior at molecular levels, including spatial arrangement of amorphous polymeric chain/fullerene in blends, has still been far from a complete understanding due to its complex nature. In 2008, two research groups reported the binary phase diagrams of semicrystalline poly(3-hexyl thiophene) (P3HT)/PCBM blends[17] and amorphous poly(phenylene vinylene) (PPV) derivative/PCBM.[18] Recently, the molecular miscibility of polymer/fullerene blends and the extent of phase separation were investigated at the molecular level.[19,20] It has also reported that PCBM molecules are intercalating between the side chains of some conjugated polymers and that this behavior influences significantly the device performance including the charge carrier transport.[21–23] More recently, it was also proved that PCBM molecules and/or their aggregates are miscible with P3HT and mobile in amorphous region of P3HT even at low temperature, 50 °C.[24]

Although charges are generally expected to be better transported in a well-ordered structure of a conjugated polymer, it has been reported that some disordered conjugated polymers[25–30] also exhibit high charge mobility in spite of their amorphous nature. Thus, it is very important to understand the charge transport mechanism in amorphous low bandgap conjugated polymer for development of high efficiency OPVs. Although several models for predicting the

[a)]Electronic mail: jungyongkim@snu.ac.kr.
[b)]Electronic mail: chlee7@snu.ac.kr.
[c)]Electronic mail: whjpoly@snu.ac.kr.

morphology of an amorphous flexible (coil-like) polymer have been developed,[31,32] the morphology of an amorphous rigid (rod-like) polymer and its blend with PCBM has not been fully studied.

With the above-mentioned point in mind, we studied the charge transport in poly(3-hexylthiophene-*alt*-6,7-dimethyl-4,9-bis-(4-hexylthien-2yl)-[1,2,5]thiadiazolo[3,4-g]quinoxaline) (P(3HT-MeTDQ)) as a model compound for amorphous conjugated rigid polymer and its blend with PCBM. Here we have employed the Gaussian disorder model (GDM) for analyzing the mobility of charge carriers, because the polymer exhibits a disordered nature.[33,34] Interestingly, through structural analysis by X-ray diffraction (XRD), we have found that amorphous P(3HT-MeTDQ) becomes partially ordered when it is blended with PCBM. This new finding recalls that poly(3-alkylthiophene)s were more organized when doped with iodine,[35] although the opposite behavior, i.e., destruction of ordering or decrease of crystallinity, has generally been expected when two materials are blended.[17,31]

II. MATERIALS AND METHODS

A. Materials

P(3HT-MeTDQ) ($M_n = 11\,100$ g/mol, $M_w = 16\,500$ g/mol, polydispersity index = 1.5, the highest occupied molecular orbital (HOMO) = −4.96 eV and LUMO = −3.79 eV by cyclic voltammetry) was synthesized by the Stille coupling polymerization.[36] PCBM was purchased from Nano-C. Poly(3,4-ethylene dioxythiophene): poly(styrene sulfonate) (PEDOT:PSS) (Baytron P VP Al 4083) was obtained from H. C. Starck.

B. Diode fabrication

A patterned indium tin oxide (ITO) glass with the sheet resistance of 10 Ω/□ was used as the substrate of device. The substrate was cleaned using acetone, isopropyl alcohol, and de-ionized water in an ultrasonic bath and then dried in an oven at 120 °C for 30 min. The 11 wt. % polymer solution (P(3HT-MeTDQ) in chlorobenzene (CB)) was spin-coated on the ITO substrate under N_2 environment in a glovebox. The thickness of the P(3HT-MeTDQ) film was 1.22 μm as measured by the atomic force microscopy (AFM). Aluminum was evaporated to deposit with 100 nm in thickness on the top of the polymer film under the pressure of $\sim 10^{-6}$ Torr. The active area of device was 2 mm^2. The diode has a typical configuration of ITO/P(3HT-MeTDQ)/Al.

C. Field effect transistor fabrication

On the top of the SiO_2 side of heavily doped *p*-type Si substrate, hexamethyldisilazane (HMDS) liquid was spin-coated sequentially at 500 rpm for 5 s and 2000 rpm for 7 s, and then a few drops of 0.5 wt. % polymer/fullerene solution (P(3HT-MeTDQ)/PCBM in CB) were spin-coated at 2000 rpm for 60 s under ambient laboratory condition. The thicknesses of spin-coated polymer/fullerene films were in the range of 20–40 nm. The blend films were annealed at 100 °C for 30 min (in the case of annealed samples). Source and drain electrodes with thicknesses of 50 nm were deposited by vacuum evaporation of Au through a shadow mask. The organic field effect transistor (OFET) has the fixed channel width (W) of 1800 μm and various lengths (L) of 40, 100, 200 and 300 μm.

D. Characterization

Molecular weight and its distribution were measured by gel permeation chromatography (GPC) (PL-GPC50) equipped with a refractive index detector using tetrahydrofuran (THF) as eluent. The columns were calibrated using standard polystyrene samples. Thermal properties were measured using differential scanning calorimetry (DSC) (TA Instruments, DSC-Q1000). Glass transition temperature (T_g) was taken as the cross point between the two tangential baselines. Optical absorption was studied by an ultraviolet-visible-near infrared (UV-vis-NIR) spectrophotometer (Lambda 850, Perkin-Elmer). XRD (X'pert Pro) was performed to examine the molecular packing of drop-cast films with ~4 μm thickness. Tapping-mode AFM images were taken with a Park systems microscope (XE-100). Transmission electron microscopy (TEM) images were obtained at 80 kV with a JSM 5410LV (JOEL). For TEM samples, P(3HT-MeTDQ)/PCBM blend films on the PEDOT:PSS/glass were immersed into de-ionized water, and the spin-coated films were then floated onto the water and collected by a 300 mesh copper grid. Mobility as a function of electric field and temperature (200–375 K) was measured using the time-of-flight photoconductivity (ToF-PC) method under the pressure of ~3 Torr. To this end, a diode fabricated as described earlier was loaded into the closed-cycle cryostat. The bias voltage of 10–80 V was applied to the device using a dc power supply (Agilent E3612A). A pulsed nitrogen laser with the wavelength of 337 nm (PTI GL-3300) was used to excite the sample. The photocurrent transient was monitored by a digital oscilloscope (Tektronix TDS 5054B). Electrical characterization of transistor was performed in the dark using a semiconductor parameter analyzer (HP 4155 C) under N_2 environment in a glovebox. Mobility was calculated in the saturated regime. The capacitance of gate dielectric (300 nm thick SiO_2 layer) was 11.8 nF/cm^2 as measured by impedance spectroscopy.

E. Density functional theory calculation

The charge transfer reorganization energy of the repeating unit of P(3HT-MeTDQ) is calculated from adiabatic potential energy surfaces of cationic and neutral form of the molecule by using the density functional theory (DFT). DFT calculation was performed at the B3LYP/6-31+(d,p) level using the Gaussian package. To make it possible to compute within feasible time, one repeating unit of the polymer was considered as a simplified model and all alkyl chains are replaced by methyl groups. In detail, to calculate the intramolecular reorganization energy, the geometries of neutral and cationic molecules were optimized. Then the energies of (a) a neutral molecule with the optimized neutral-molecule structure, (b) a neutral molecule with the optimized cation structure, (c) a cation with the optimized cation structure, and (d) a cation with the optimized neutral-molecule structure were calculated. Finally, from these four energies, the

reorganization energy could be obtained (see Fig. 1 of the supplemental material).[37]

III. RESULTS AND DISCUSSION

A. Characterization of a low bandgap polymer

P(3HT-MeTDQ) is an alternating copolymer designed for better harvesting of the solar photon flux, as shown in Fig. 1(a).[36] It is composed of D-A-D building blocks, in which A is an electron-deficient methyl thiadiazolo quinoxaline (TDQ) and D is an electron-rich hexyl thiophene. The UV-vis-NIR absorption spectrum of P(3HT-MeTDQ) shows a typical bimodal shape, as shown in Fig. 1(b), where the absorption at a shorter wavelength arises from the D unit and the absorption at a longer wavelength arises from the internal charge transfer between D and A units in the copolymer, as observed in other D/A-type copolymers with similar chemical structure.[3,4,38] The absence of vibronic absorption indicates a disordered nature of the polymer.

The HOMO ($=-4.65$ eV), LUMO ($=-3.27$ eV) and intramolecular reorganization energy ($\lambda = 0.31$ eV) of the repeating unit (3HT-MeTDQ) were calculated from adiabatic potential energy surfaces of cationic and neutral form of the molecule by using DFT (see Fig. 1 in the supplemental material).[8,37,39–44] It should be noted here that the reorganization energies of organic molecules calculated from potential energy surface are nearly the same as those from the normal mode expansion.[42] The HOMO/LUMO wave functions shown in Figs. 1(c) and 1(d) reveal that the LUMO wave function is mostly localized on the TDQ site, whereas the HOMO one is uniformly delocalized along the structural unit, indicating that electrons may not be easily transported along the polymer backbone due to energetic barrier.

As M_n of P(3HT-MeTDQ) is 11 100 g/mol, the density of chain end sites (δ_{ES}) is estimated $\sim 1.1 \times 10^{20}\,\mathrm{cm}^{-3}$ according to the relation, $\delta_{ES}(\mathrm{cm}^{-3}) = 10^{24.1}/M_n$, which is formulated on the following assumptions: (1) the polymer density is $1\,\mathrm{g/cm}^3$ and (2) one chain has two end sites. Considering that the density of electronically active impurity in most of organic semiconductors is 10^{15}–$10^{17}\,\mathrm{cm}^{-3}$, the δ_{ES} value of P(3HT-MeTDQ) is so large that the chain end site acts as a defect for charge transport.[45]

The XRD pattern for drop-cast P(3HT-MeTDQ) film on HMDS-coated silicon substrate is shown in Fig 2 of the supplemental material.[37] In this experiment, we adopted the thin-film experimental technique to increase the sensitivity of XRD: X rays were irradiated onto a film at a fixed low angle ($=0.5°$), simultaneously the diffracted beam was recorded at 2θ degree in out-of-plane direction. A weak and broad peak was observed at $2\theta = 21.5°$ ($d = 4.1$ Å), which is tentatively assigned as the average distance between parallel neighboring π-stacking. Therefore, the XRD pattern leads us to conclude that P(3HT-MeTDQ) has a small ordering of polymer chains in an amorphous phase. However, when we examined the crystallinity by using DSC, the thermogram does not show a melting transition in the temperature range of 193–573 K, whereas it weakly shows a T_g at 285 K (see Fig. 3 in the supplemental material).[37] This T_g value is slightly higher than those of regioregular (*rr*) P3HT ($T_g = 259$ K) and regiorandom P3HT ($T_g = 280$ K).[17]

The AFM height and corresponding phase lag images for the spin-coated P(3HT-MeTDQ) film show some nodular aggregates with a size of several tens of nanometers (see Fig.

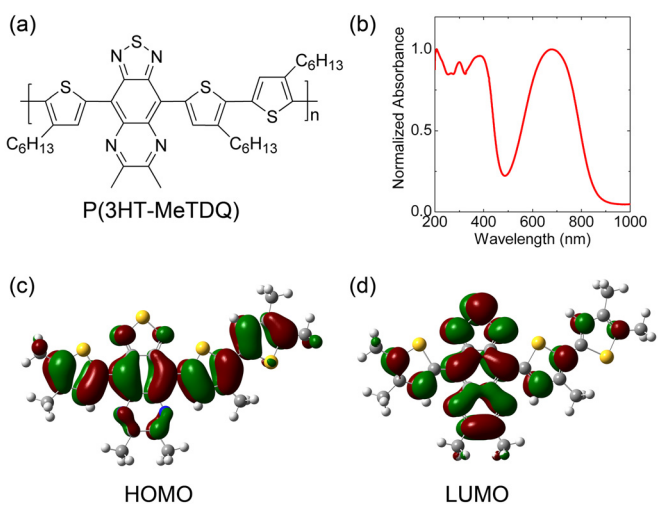

FIG. 1. (Color online) (a) Chemical structure of P(3HT-MeTDQ). (b) UV-vis-NIR absorption spectra of P(3HT-MeTDQ) film. (c) HOMO ($=-4.65$ eV) and (d) LUMO ($=-3.27$ eV) of the repeating unit of P(3HT-MeTDQ), which are calculated using the density functional theory.

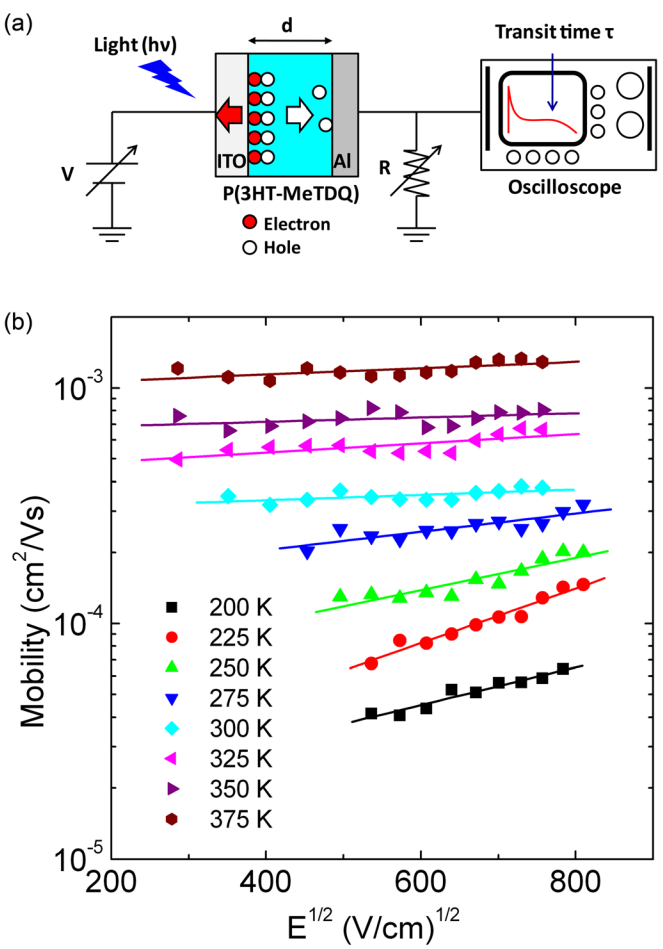

FIG. 2. (Color online) (a) Experimental setup of ToF-PC and (b) the hole mobility in P(3HT-MeTDQ) as a function of electric field at various temperatures.

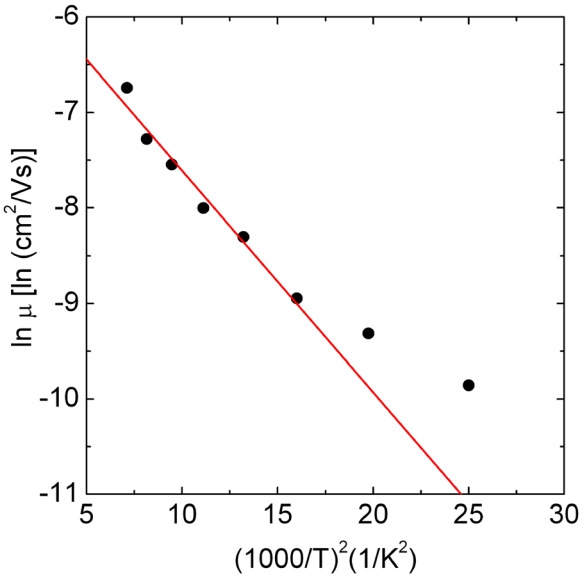

FIG. 3. (Color online) The plot of zero field hole mobility vs $1/T^2$. The film thickness of P(3HT-MeTDQ) is 1.22 μm.

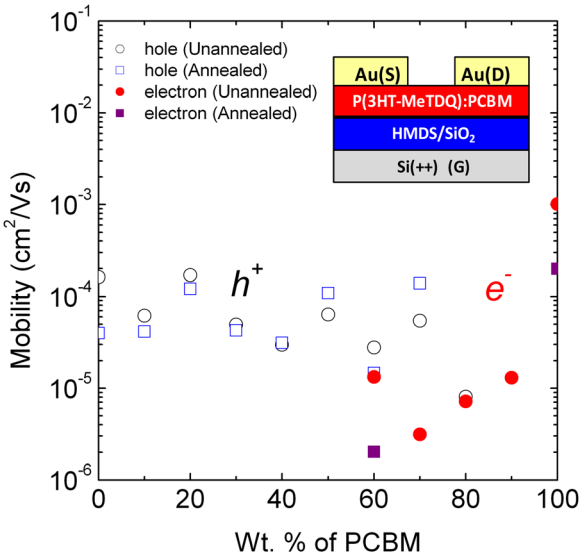

FIG. 4. (Color online) Charge mobility as a function of the PCBM content at 300 K with $L = 40\,\mu$m and $W = 1800\,\mu$m. Circle and square symbols denote unannealed and annealed samples, respectively. Inset represents the FET architecture with a semiconducting layer of P(3HT-MeTDQ)/PCBM.

4 of the supplemental material),[37] whereas the semicrystalline *rr*-P3HT shows a fibril structure arising from the bundle of stacked chains or lamellae, indicating that P(3HT-MeTDQ) is amorphous in solid state. A TEM image [see Fig. 4(c) of the supplemental material][37] also confirms the AFM image. In short, the results of XRD, DSC, AFM, and TEM lead us to conclude that P(3HT-MeTDQ) is an amorphous material with partial molecular ordering.

B. Charge transport in low bandgap polymer

Figure 2(a) shows an experimental setup of ToF-PC for measuring the charge drift mobility. The devices were fabricated with the ITO/P(3HT-MeTDQ)/Al configuration. Briefly describing, a light pulse with higher energy than the polymer bandgap was irradiated on the semitransparent ITO electrode for a short time, and then the transit time (t) of photogenerated charge carriers was measured. The transit time of charge carrier was determined at the intersection of asymptotes to the plateau and the tailing edge of the photocurrent transient (see Figs. 5 and 6 of the supplemental material).[37] Then the charge mobility (μ) is determined using the following relation:

$$\mu = \frac{d}{E \cdot t} = \frac{d^2}{V \cdot t}, \tag{1}$$

where d, E, and V are the thickness of film, an electric field, and an applied voltage, respectively.[33,34] The calculated hole mobility (μ_h) of P(3HT-MeTDQ) is 3.4×10^{-4} cm^2/V s at 300 K when the value of $d = 1.22\,\mu$m, $E = 410$ kV/cm, and $t = 0.89\,\mu$s are used for Eq. (1).[46–48]

When the logarithm of hole mobility in P(3HT-MeTDQ) film is plotted against the square root of electric field in the temperature range of 200–375 K, as shown in Fig. 2(b), it is realized that the slope of the plot decreases gradually with increasing the temperature up to 275 K. However, the mobility becomes almost independent of the electric field as the temperature is higher than the T_g (=285 K) of P(3HT-MeTDQ). A similar behavior was also observed in *rr*-P3HT film.[49] This is probably because the phonon-assisted charge hopping is readily available above T_g due to active segmental motions of polymer chains, whereas the polymer chains are frozen below T_g except for local vibrational motions of side groups and chain ends.[50,51]

When the charge mobility in π-conjugated polymers (amorphous or semicrystalline state) is thermally activated,

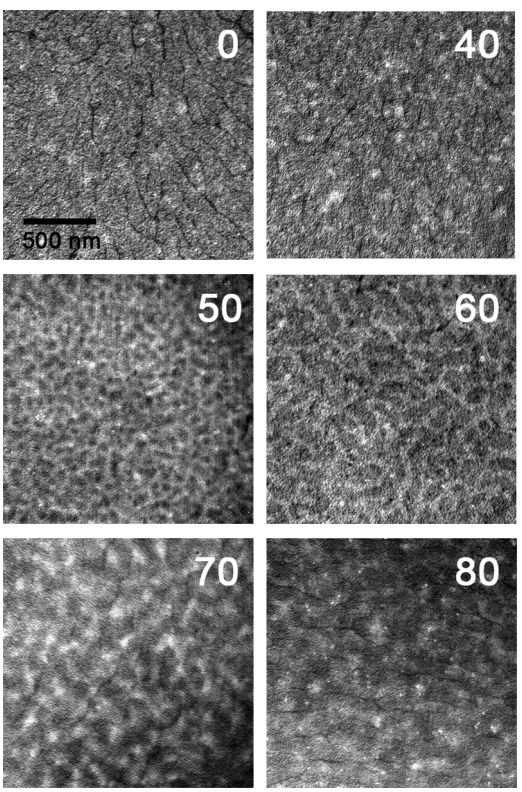

FIG. 5. TEM images of P(3HT-MeTDQ)/PCBM blend films with various compositions (wt. %).

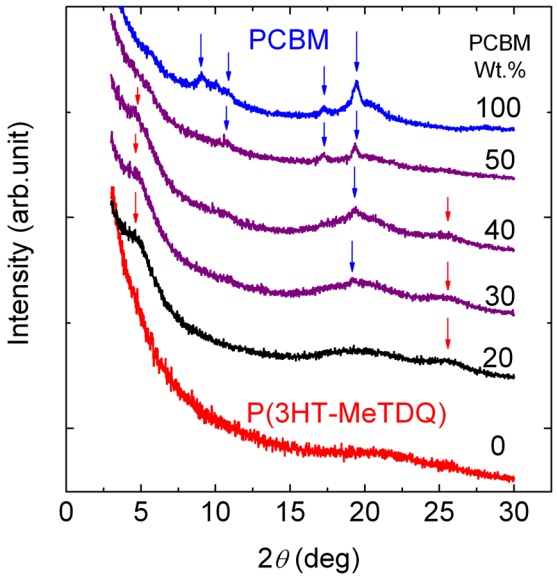

FIG. 6. (Color online) XRD patterns of drop-cast P(3HT-MeTDQ)/PCBM films with 4 μm. All samples were annealed at 100°C for 30 min.

it can be described by a hopping transport model, so called the GDM,

$$\mu(E,T) = \mu_\infty \exp\left[-\left(\frac{2\sigma}{3k_BT}\right)^2\right] \exp\left\{C\sqrt{E}\left[\left(\frac{\sigma}{k_BT}\right)^2 - \Sigma^2\right]\right\}, \quad (2)$$

where T, μ_∞, k_B, C, σ, and Σ are temperature, the mobility at high temperature limit, the Boltzmann constant, an empirical constant, energetic disorder, and positional disorder (i.e., off-diagonal disorder), respectively.[33] This model is generally valid because it has been known that the mobility is dependent on the electric field and the temperature with the specific relations of $\mu \propto \exp(\sqrt{E})$ and $\mu \propto \exp(1/T^2)$ in many organic semiconductors.[34,52] A value of $\sigma = 62$ meV was obtained for P(3HT-MeTDQ) from the slope of the plot in Fig. 3, $\partial \ln \mu(0,T)/\partial(1/T^2) = -(2\sigma/3k_B)^2$. This value representing the Gaussian distribution width of site energy in P(3HT-MeTDQ) is much smaller than those ($\sigma = 93$–112 meV) of well-known amorphous PPV derivatives.[53] A prototypical amorphous polymer, poly(2-methoxy-5-(3′,7′-dimethyloctyloxy)-*p*-phenylenevinylene) with M_n of 23 000 g/mol was reported to have a hole mobility of $\sim 10^{-7}$ cm^2/V s,[23] which is three orders of magnitude lower than that of P(3HT-MeTDQ) with M_n of 11 100 g/mol. This much higher mobility (3.4×10^{-4} cm^2/V s at 300 K) in P(3HT-MeTDQ) may arise from a lower σ value owing to its rigid structure with fused ring thiophene.[54,55] As the chain rigidity of polymer is well represented by its persistence length,[56] we calculated the persistence lengths of P(3HT-MeTDQ) and *rr*-P3HT and compared with each other. The larger the persistence length, the more rigid the chain backbone, because the persistence length is a measure of how far along the backbone one has to go before the orientation changes. For the calculation of persistence length, molecular dynamics simulation was conducted for 10 ns with a time step of 1 fs based on the worm-like chain model by using AMBER9 package with a generalized AMBER force field. The calculated persistence lengths of P(3HT-MeTDQ) and *rr*-P3HT are 19.3 and 12.3 nm, respectively, indicating that P(3HT-MeTDQ) is more rigid than P3HT. Another noteworthy point from Fig. 3 is that a transition takes place around 250 K. It is generally accepted that the transport mechanism changes from non-dispersive to dispersive one at the transition temperature (T_c), when a change is observed in the slope of the plot of $\ln \mu$ vs $1/T^2$.[33]

It has been known that the GDM is applicable in the range of temperature ($T_c < T < T_g$).[34] Although the corresponding range for P(3HT-MeTDQ) is 250 K $< T <$ 285 K, the theory also describes well the zero field mobility of P(3HT-MeTDQ) at the temperature as high as 375 K. This is probably because the rigid chain backbone has only limited segmental motions up to 375 K. When the activation energy (ΔE_a) is determined from the slope of the Arrhenius plot, $\ln \mu$ vs $1/T$, it is realized that ΔE_a is dependent on the electric field, i.e., ΔE_a decreases from 124 to 108 meV as E increases from 290 to 570 kV/cm.[57] This is because the potential energy barrier is reduced in the direction of the electric field, as expected from the Poole–Frenkel theory.[52] It is noted that ΔE_a represents the external thermal energy required for the charge carriers to overcome this potential barrier and hop to another site.[58]

The β value {$=C[(\sigma/k_BT)^2 - \Sigma^2]$ in Eq. (2)} is obtained from the slope of $\partial \ln \mu(E,T)/\partial\sqrt{E}$. When β is plotted against $(2\sigma/k_BT)^2$, the values of $C = 2.3 \times 10^{-4}$ (cm/V^2)$^{1/2}$ and $\Sigma = 1.7$ for P(3HT-MeTDQ) are obtained from the slope and intercept of the plot, respectively. Note that the values of P(3HT-MeTDQ) are comparable to the values of *rr*-P3HT ($C = 1.5 \times 10^{-4}$ (cm/V^2)$^{1/2}$ and $\Sigma = 3.4$) reported by Mozer *et al.*[59] This may explain the reason why the hole mobility of P(3HT-MeTDQ) is comparable to that of *rr*-P3HT although the former is an amorphous material, whereas the latter is a semicrystalline polymer. The hole mobilities of unannealed P(3HT-MeTDQ) are 3.4×10^{-4} cm^2/V s at 370 kV/cm (ToF) and 1.6×10^{-4} cm^2/V s [field effect transistor (FET)] at 300 K, which are comparable to the values of *rr*-P3HT film (5×10^{-4} cm^2/V s at 394 kV/cm (ToF) and 4.4×10^{-4} cm^2/V s (FET) at $T = 300$ K) prepared under the same processing condition.

C. Charge transport and phase behavior in amorphous low bandgap polymer/fullerene blends

Charge transport in a transistor made of a P(3HT-MeTDQ)/PCBM blend was examined to estimate the relation between charge carrier mobility and phase morphology. The device structure in this study is shown in the inset of Fig. 4. Contact resistance of FET devices is represented in detail (see Figs. 7 and 8 of the supplemental material).[37] When the blend ratio of polymer/fullerene was systematically varied, it was observed that the ambipolar transport starts to occur at 60 wt. % PCBM, as shown in Fig. 4, indicating that electrically bicontinuous network is formed at the 60 wt. % PCBM. The formation of bicontinuous network is essential for a high efficiency OPV device. It should be noted that this composition is almost the same as that of the best performing solar cell (67 wt. % PCBM) reported in our previous work.[36] The hole

and electron mobilities in an OFET device with 60–70 wt. % PCBM were $\mu_h = 2.8–5.4 \times 10^{-5}$ cm^2/V and $\mu_e = 1.3–0.3 \times 10^{-5}$ $cm^2/V\,s$, respectively, whereas the mobilities in an OPV device with 67 wt. % PCBM were $\mu_h = 6.4 \times 10^{-6}$ cm^2/V and $\mu_e = 1.1 \times 10^{-5}$ $cm^2/V\,s$ as measured by the dark injection space charge limited current method.[36] The difference of charge mobility between OFET and OPV is within an order of magnitude, which arises from different processing conditions, device geometry, and charge concentration ($\sim 10^{19}\,cm^{-3}$ (OFET) vs $\sim 10^{16}\,cm^{-3}$(OPV)).[60]

Another feature to be noted from Fig. 4 is that the hole mobility slowly decreases from 1.6×10^{-4} $cm^2/V\,s$ (0 wt. % PCBM) to 8.1×10^{-6} $cm^2/V\,s$ (80 wt. % PCBM) for unannealed device, whereas the electron mobility starts to be observed at 60 wt. % PCBM as the PCBM network increases. However, as the PCBM content is increased further, the electron mobility decreases first and then increases, showing a minimum at 70 wt. % PCBM.

Hole mobility of an annealed device slightly increases from 4.0×10^{-5} $cm^2/V\,s$ (0 wt. %) to 1.4×10^{-4} $cm^2/V\,s$ (70 wt. %) as the PCBM content increases, whereas ambipolar transport is observed at 60 wt. %, as shown in Fig. 4. This indicates that annealing does not induce network formation of the PCBM phase at the composition <60 wt. %. Particularly, electron mobility cannot be measured experimentally in the range of 70–90 wt. % PCBM, indicating that PCBM is macroscopically phase-separated upon annealing where electrons may easily be trapped in PCBM domains.[14,15] Comparison of charge mobility of an unannealed device with that of an annealed one indicates that annealing does not enhance charge mobility for amorphous conjugated polymer P(3HT-MeTDQ).

The charge transport properties of polymer/fullerene blends are closely related to the morphological structures of blends. As shown in Fig. 5, the TEM image of 40 wt, % PCBM blend looks very similar to the image of pure polymer (0 wt. % PCBM). But, the image of 50 wt. % PCBM blend clearly shows dark islands in a white sea, where dark islands correspond to phase-separated PCBM domains because PCBM nanocrystals have higher electron density. By increasing further the PCBM concentration in blend, we now clearly observe pseudo-bicontinuous network at 60 wt. % PCBM where ambipolar transport is observed, whereas the films with 70–80 wt. % PCBM show that they are macroscopically phase-separated.

Another sensitive tool to characterize the phase behavior of conjugated polymer/fullerene at the molecular level is to use XRD. To more clearly observe the XRD pattern, the film was prepared by drop-cast and annealed at 100 °C for 30 min, as the drop-casting method allows a solvent to evaporate slowly and thus provides a better chance for the components to self-aggregate. Further annealing may provide more opportunity for components to self-organize. Although the diffraction peaks of PCBM crystal are clearly observed at $2\theta = 9.1$, 10.1, 10.8, and 19.5° for a 100% PCBM sample, as shown in Fig. 6, the samples with 30–40 wt. % PCBM show only the primary peak of PCBM at $2\theta = 19.5°$ with other weaker peaks arising presumably from P(3HT-MeTDQ). At 20 wt. % PCBM, the PCBM peak is not discernable.

We observed a very interesting phenomenon in XRD patterns: For the samples with 20–40 wt. % PCBM, a broad peak was observed at $2\theta = 5°$ (d-spacing = 17.7 Å), which does not come from PCBM, whereas the pure polymer P(3HT-MeTDQ) (0% PCBM) did not show a discernable peak at $2\theta = 5°$ in the XRD pattern. The diffraction peak at $2\theta = 5°$ ($d = 17.7$ Å) has been assigned as the interchain distance from the analogy of the interchain distance ($d = 16.5$ Å) of the crystal structure of *rr*-P3HT[17,61] and low bandgap copolymer.[62] Further, for the samples with 20–40 wt. % PCBM, a very broad bump was observed at $2\theta = 25.5°$, as shown in Fig. 6. It is strongly possible that this broad peak arises from a broad distribution of π-stacking of polymer chains with $d = 3.5$ Å. Considering that a *rr*-P3HT/PCBM blend exhibits sharper and stronger π-stacking peak at $2\theta = 23°$($d = 3.86$ Å) as compared to that of P(3HT-MeTDQ), *rr*-P3HT has much highly ordered π-stacking than P(3HT-MeTDQ).[17] Nevertheless, the charge mobilities of P(3HT-MeTDQ) are comparable to those of *rr*-P3HT, as discussed previously. Therefore, we believe that partial ordering of P(3HT-MeTDQ) contributes significantly to the hole mobility in blend films (higher than 10^{-5} $cm^2/V\,s$). To the best of our knowledge, an enhanced ordering of conjugated polymer after blending with PCBM is the first finding among amorphous conjugated polymer/fullerene systems.

IV. CONCLUSIONS

When the charge transport behavior in an amorphous low bandgap polymer (P(3HT-MeTDQ)) was analyzed using the GDM, the polymer has the values of $\sigma = 62$ meV, $\Sigma = 1.7$, and $C = 2.3 \times 10^{-4}$ $(cm/V^2)^{1/2}$, which are comparable to those of semicrystalline *rr*-P3HT. The high hole mobility of $\sim 10^{-4}$ $cm^2/V\,s$ in amorphous P(3HT-MeTDQ) likely originates from the following contributions (1) the small energetic and positional disorder, (2) the intra-/interchain π-electron delocalization through the planar structure of the main chain, and (3) the relatively small reorganization (0.31 eV) and polarization energies owing to the planar structure of the rigid chain. In P(3HT-MeTDQ)/PCBM blends, the formation of a bicontinuous network was identified at 60 wt. % PCBM by TEM, at which the charge transport switched from hole-only to ambipolar transport. Interestingly, we have found that the amorphous P(3HT-MeTDQ) becomes partially ordered when it is blended with PCBM, as evidenced by observation of discernible XRD peaks at $2\theta = 5°$ ($d = 17.7$ Å) and 25.5° ($d = 3.5$ Å), corresponding to the interchain distance and π-stacking distance, respectively.

ACKNOWLEDGMENTS

The authors thank the Ministry of Education, Science and Technology (MEST), Korea for financial support through the Global Research Laboratory (GRL), Acceleration Research (R0 A-2008-000-20108-0), and BK21 programs.

[1]G. Yu, J. Gao, J. C. Hummelen, F. Wudl, and A. J. Heeger, Science, **270**, 1789 (1995).
[2]J. J. M. Halls, C. A. Walsh, N. C. Greenham, E. A. Marsegila, R. H. Friend, S. C. Moratti, and A. B. Holmes, Nature (London) **376**, 498 (1995).

[3]N. Blouin, A. Michaud, D. Gendron, S. Wakim, E. Blair, R. Neagu-Plesu, M. Belletete, G. Durocher, Y. Tao, and M. Leclerc, J. Am. Chem. Soc. **130**, 732 (2008).
[4]Z. Zhu, D. Waller, and C. J. Brabec, *Organic Photovoltaics: Materials, Device Physics, and Manufacturing Technologies*, edited by C. J. Brabec, V. Dyakonov, and U. Scherf (Wiley-VCH, Weinheim, 2008).
[5]H.-Y. Chen, J. Hou, S. Zhang, Y. Liang, G. Yang, Y. Yang, L. Yu, Y. Wu, and G. Li, Nature Photon., **3**, 649 (2009).
[6]Y. Liang and L. Yu, Acc. Chem. Res., **43**, 1227 (2010).
[7]M. C. Scharber, D. Muehlbacher, M. Koppe, P. Denk, C. Waldauf, A. J. Heeger, and C. J. Brabec, Adv. Mater. **18**, 789 (2006).
[8]J. L. Brédas, D. Beljonne, V. Coropceanu, and J. Cornil, Chem. Rev. **104**, 4971 (2004).
[9]R. Marcus, Angew. Chem. Int. Ed. Engl. **32**, 1111 (1993).
[10]D. Hertel and H. Bässler, Chem. Phys. Chem. **9**, 666 (2008).
[11]G. Dennler, M. C. Scharber, and C. J. Brabec, Adv. Mater. **21**, 1323 (2009).
[12]B. A. Gregg, J. Phys. Chem. C **113**, 5899 (2009).
[13]L. G. Kaake, P. F. Barbara, and X. Y. Zhu, J. Phys. Chem. Lett. **1**, 628 (2010).
[14]X. Yang and J. Loos, Macromolecules **40**, 1353 (2007).
[15]D. Venkataraman, S. Yurt, B. H. Venkatraman, and N. Gavvalapalli, J. Phys. Chem. Lett. **1**, 947 (2010).
[16]E. Verploegen, R. Mondal, C. J. Bettinger, S. Sok, M. F. Toney, and Z. Bao, Adv. Funct. Mater. **20**, 3519 (2010).
[17]J. Y. Kim and C. D. Frisbie, J. Phys. Chem. C **112**, 17726 (2008).
[18]C. Muller, T. A. M. Ferenczi, M. Campoy-Quiles, J. M. Frost, D. D. C. Bradley, P. Smith, N. Stingelin-Stutzmann, and J. Nelson, Adv. Mater. **20**, 3510 (2008).
[19]R. C. Nieuwendaal, C. R. Snyder, J. Kline, E. K. Lin, D. L. VanderHart, and D. M. Delongchamp, Chem. Mater. **22**, 2930 (2010).
[20]B. A. Collins, E. Gann, L. Guignard, X. He, C. R. Mcneill, and H. Ade, J. Phys. Chem. Lett. **1**, 3160 (2010).
[21]A. C. Mayer, M. F. Toney, S. R. Scully, J. Rivnay, C. J. Brabec, M. Scharber, M. Koppe, M. Heeney, I. McCulloch, and M. D. McGehee, Adv. Funct. Mater. **19**, 1173 (2009).
[22]N. C. Cates, R. Gysel, Z. Beiley, C. E. Miller, M. F. Toney, M. Heeney, I. McCulloch, and M. D. McGehee, Nano Lett. **9**, 4153 (2009).
[23]N. C. Cates, R. Gysel, J. E. P. Dahl, A. Sellinger, and M. D. McGehee, Chem. Mater. **22**, 3543 (2010).
[24]N. D. Treat, M. A. Brady, G. Smith, M. F. Toney, E. J. Kramer, C. J. Hawker, and M. L. Chabinyc, Adv. Energy Mater. **1**, 82 (2011).
[25]D. Mühlbacher, M. Scharber, M. Morana, Z. Zhu, D. Waller, R. Gaudiana, and C. J. Brabec, Adv. Mater. **18**, 2884 (2006).
[26]N. Blouin, A. Michaud, and M. Leclerc, Adv. Mater. **19**, 2295 (2007).
[27]X. Zhan, Z. Tan, B. Domercg, Z. An, X. Zhang, S. Barlow, Y. Li, D. Zhu, B. Kippelen, and S. R. Marder, J. Am. Chem. Soc. **129**, 7246 (2007).
[28]H. Yan, Z. Chen, Y. Zheng, C. Newman, J. Quinn, F. Dötz, M. Kastler, and A. Facchetti, Nature (London) **457**, 679 (2009).
[29]J. Veres, S. D. Ogier, S. W. Leeming, D. C. Cupertino, and S. M. Khaffaf, Adv. Funct. Mater. **13**, 199 (2003).
[30]J. Veres, S. D. Ogier, G. Lloyd, and D. de Leeuw, Chem. Mater. **16**, 4543 (2004).
[31]P. J. Flory, *Principles of Polymer Chemistry* (Cornell University Press, Ithaca, NY, 1953).
[32]G. S. Y. Yeh, J. Macromol. Sci. Phys. **B6**, 465 (1972).
[33]H. Bässler, Phys. Status Solidi B **175**, 15 (1993).
[34]P. M. Borsenberger and D. S. Weiss, *Organic Photoreceptors for Xerography* (Marcel Dekker, New York, 1998).
[35]K. Tashiro and M. Kobayashi, Polymer **38**, 2867 (1997).
[36]Y. Lee, T. P. Russell, and W. H. Jo, Org. Electron. **11**, 846 (2010).
[37]See supplementary material at http://dx.doi.org/10.1063/1.3686633 for reorganization energy, XRD, DSC, AFM, TEM, photocurrent transient data, the current–voltage characteristic and contact resistance for transistors, and Figures 1–8.
[38]P. M. Beaujuge, C. M. Amb, and J. R. Reynolds, Acc. Chem. Res. **43**, 1396 (2010).
[39]M. J. Frisch, G. W. Trucks, H. B. Schlegel *et al.*, GAUSSIAN 03, Revision B.03, Gaussian, Inc., Pittsburgh, PA, 2003.
[40]A. D. Becke, J. Chem. Phys. **98**, 5648 (1993).
[41]E. G. Kim, V. Coropceanu, N. E. Gruhn, R. S. Sanchez-Carrera, R. Snoeberger, A. J. Matzger, and J.-L. Brédas, J. Am. Chem. Soc. **129**, 13072 (2007).
[42]S. S. Zade and M. Bendikov, Chem. Eur. J. **14**, 6734 (2008).
[43]S. S. Zade, N. Zamoshchik, and M. Bendikov, Acc. Chem. Res. **44**, 14 (2011).
[44]The intramoleuclar reorganization energies for 4-mers and 6-mers of thiophene were calculated for comparison purpose, which are 0.28 and 0.25 eV, respectively, which are very consistent with the λ values reported by Zade and Bendikov in Ref. 42, in which λ changes from 0.4 eV (monomer) to 0.25 eV (6-mers). It should be noted here that the variation must not be large although the value of λ decreases with increasing the chain length (Refs. 42 and 43).
[45]A. W. Hains, Z. Liang, M. A. Woodhouse, and B. A. Gregg, Chem. Rev. **110**, 6689 (2010).
[46]A. M. Ballantyne, J. S. Wilson, J. Nelson, D. D. C. Bradley, J. R. Durrant, M. Heeney, W. Duffy, and I. McCulloch, Proc. SPIE **6334**, 633408 (2006).
[47]A. J. Morfa, A. M. Nardes, S. E. Shaheen, N. Kopidakis, and J. van de Largemaat, Adv. Funct. Mater. **21**, 2580 (2011).
[48]In this work, the film thickness was fixed to 1.22 μm. One who has interest in the thickness dependence of ToF photoconductivity can refer to the literature (Refs. 46 and 47), in which a commercially available P3HT was studied in detail.
[49]In a *rr*-P3HT film, the hole mobility is also independent of the electric field as the temperature is higher than $T_g = 259$ K of polymer.
[50]O. Olabisi, L. M. Robeson, and M. T. Shaw, *Polymer-Polymer Miscibility* (Academic, New York, 1979).
[51]L. H. Sperling, *Introduction to Physical Polymer Science* (Wiley, New York, 1993).
[52]J. Frenkel, Phys. Rev. Lett. **54**, 647 (1938).
[53]H. C. F. Martens, P. W. M. Blom, and H. F. M. Schoo, Phys. Rev. Lett. **61**, 7489 (2000).
[54]P. Coppo and M. L. Turner, J. Mater. Chem. **15**, 1123 (2005).
[55]M. Zhang, H. N. Tsao, W. Pisula, C. Yang, A. K. Mishra, and K. Müllen, J. Am. Chem. Soc. **129**, 3472 (2007).
[56]P. C. Hiemenz, and T. P. Lodge, *Polymer Chemistry* (CRC Press, Boca Raton, FL, 2007).
[57]A. Pivrikas, M. Ullah, H. Sitter, and N. S. Sariciftci, Appl. Phys. Lett. **98**, 092114 (2011).
[58]M. Pope and C. E. Swenberg, *Electronic Processes in Organic Crystals and Polymers* (Oxford University Press, New York, 1999).
[59]A. J. Mozer, N. S. Sariciftci, A. Pivrikas, R. Osterbacka, G. Juska, L. Brassat, and H. Bässler, Phys. Rev. B **71**, 035214 (2005).
[60]C. Tanase, E. J. Meijer, P. W. M. Blom, and D. M. de Leeuw, Phys. Rev. Lett. **91**, 216601 (2003).
[61]H. Sirringhaus, P. J. Brown, R. H. Friend, M. M. Nielsen, K. Bechgaard, B. M. W. Langevel-Voss, A. J. H. Spiering, R. A. Janssen, E. W. Meijer, P. Herwig, and D. M. de Leew, Nature (London) **401**, 685 (1999).
[62]P. M. Beaujuge, W. Pisula, H. N. Tsao, S. Ellinger, K. Müllen, and J. R. Reynolds, J. Am. Chem. Soc. **131**, 7514 (2009).